Electron spin dynamics and electron spin resonance in graphene

B. Dóra[1], F. Murányi[2] and F. Simon[1,3(a)]

[1] *Budapest University of Technology and Economics, Institute of Physics and Condensed Matter Research Group of the Hungarian Academy of Sciences - H-1521 Budapest, Hungary, EU*
[2] *Physik-Institut der Universität Zürich - Winterthurerstr. 190, CH-8057 Zürich, Switzerland*
[3] *Universität Wien, Fakultät für Physik - Strudlhofgasse 4, 1090 Wien, Austria, EU*

Abstract – A theory of spin relaxation in graphene including intrinsic, Bychkov-Rashba, and ripple spin-orbit coupling is presented. We find from spin relaxation data by Tombros *et al.* (*Nature*, **448** (2007) 571) that intrinsic spin-orbit coupling dominates over other contributions with a coupling constant of 3.7 meV. Although it is 1–3 orders of magnitude larger than those obtained from first principles, we show that comparable values are found for other honeycomb systems, MgB_2 and LiC_6; the latter is studied herein by electron spin resonance (ESR). We assess the feasibility of bulk electron spin resonance spectroscopy on graphene and identify experimental conditions where such experiments are realizable.

Introduction. – The discovery of graphene [1] stimulated enormous interest due its fundamentally and technologically important properties. One potential application is in spintronics [2], *i.e.* when the electron spin degree of freedom is utilized as information carrier. The principal parameter governing spintronic usability is the spin relaxation time (also referred to as spin-lattice relaxation time), τ_s, which characterizes how an injected non-thermal equilibrium spin state decays. For realistic applications, τ_s longer than 10–100 ns is required. A general, often cited concept is that "pure materials made of light elements" can reach this limit. The huge mobility of charge carriers in graphene (approaching 10^6 cm^2/V s [3]), the light nature of carbon, and the low-dimensionality of this material are the reasons for the high expectations for its spintronic applications. This is supported by the long spin relaxation time in light metals such as, *e.g.*, Li [4] or in low-dimensional conductors [5].

Therefore it came as a surprise that τ_s as short as 60–150 ps are observed in spin transport experiments on graphene [6,7], which renders it unusable for such applications. The understanding of this experimental result is therefore of great importance. Theories of spin relaxation are split into two different classes: materials with inversion symmetry (*e.g.*, Na or Si) and materials where the inversion symmetry is broken either in the

bulk (*e.g.*, III–V semiconductors such as GaAs) or in two-dimensional heterostructures. The Elliott-Yafet (EY) theory [8,9] explains the former case, where only intrinsic (*i.e.*, atomic) spin-orbit coupling (SOC) is present, L_i, and predicts that spin ($\Gamma_s = \hbar/\tau_s$) and momentum relaxation rates ($\Gamma = \hbar/\tau$, τ is the momentum relaxation time) are proportional: $\Gamma_s = \alpha_i \frac{L_i^2}{\Delta^2}\Gamma$. Here $\alpha_i = 1, \ldots, 10$ is band structure dependent [4], Δ is the energy separation of a neighboring and the conduction band.

The relaxation for broken inversion symmetry is explained by the Dyakonov-Perel (DyP) theory. It applies either when the symmetry breaking is in the bulk (the Dresselhaus SOC [10], L_D) or when it happens for a heterolayer structure (the Bychkov-Rashba SOC [11,12], L_{BR}). The DyP theory shows that the spin and momentum relaxation rates are inversely proportional: $\Gamma_s = \alpha_{D/BR} L_{D/BR}^2/\Gamma$, where $\alpha_{D/BR} \approx 1$.

A link between the EY and the DyP was found recently [13]: for metals with inversion symmetry but rapid momentum scattering, the generalization of the EY theory leads to $\Gamma_s = \alpha_i \frac{L_i^2}{\Delta^2+\Gamma^2}\Gamma$, which gives a DyP-like spin relaxation when $\Gamma > \Delta$.

Three sources of SOC are present in graphene: intrinsic, BR type (due to the symmetry breaking by a perpendicular electric field), and the ripple related (which is due to the inevitable ripples in graphene). However, the role and magnitude of these SOC parameters is a debated

[(a)]E-mail: `ferenc.simon@univie.ac.at`

issue. Estimates for the intrinsic SOC ranges two orders of magnitude; 0.9–$200\,\mu\text{eV}$ [14–16], whereas the value of the BR SOC appears to be settled to 10–$36\,\mu\text{eV}$ per V/nm (refs. [15] and [14], respectively). Alternative scenarios for the anomalous spin-relaxation such as the effect of the substrate [17] and impurities [18] were also suggested.

Here, we present the theory of spin relaxation in graphene including intrinsic, BR, and ripple spin-orbit coupling. We analyze the spin transport data from refs. [6,7,19] and we find that the intrinsic SOC dominates the relaxation with a large, unexpected magnitude. We discuss two similar honeycomb systems: MgB_2 and LiC_6, and show that they exhibit similar intrinsic SOC. The result predicts a strong anisotropy of the spin relaxation time. We study the feasibility of bulk electron spin resonance (ESR) spectroscopy on graphene and pinpoint experimental conditions when it is possible. ESR would allow a direct, spectroscopic measurement of τ_s (ref. [20]), which underlines its importance [21].

Experimental. – We prepared Li-intercalated HOPG graphite by the "immersion into molten Li" method [22]. The golden color of the samples attested the LiC_6 intercalation level [23]. Freshly cleaved samples were sealed under He in quartz tubes for the ESR experiment.

Spin relaxation in graphene. – Low-energy excitations around the K point of the Brillouin zone are described by a two-dimensional Dirac equation:

$$H = v_\text{F}(\sigma_x p_x + \sigma_y p_y), \qquad (1)$$

with the $v_\text{F} \approx 10^6\,\text{m/s}$ Fermi velocity [1]. The spin-orbit interaction in graphene is given by [14]

$$H_\text{SO} = L_\text{i}\sigma_z S_z + \frac{L_\text{BR} + L_\text{ripple}(\mathbf{r})}{2}(\sigma_x S_y - \sigma_y S_x), \quad (2)$$

where L_i, L_BR, and L_ripple are the SOCs of the intrinsic, BR, and ripple terms, respectively. $L_\text{ripple}(\mathbf{r})$ is a Gaussian correlated random variable, $\langle L_\text{ripple}(\mathbf{r})L_\text{ripple}(\mathbf{r}')\rangle \sim \delta(\mathbf{r} - \mathbf{r}')$.

The spin relaxation rates induced by these SOCs are additive in lowest order provided $\max(L_\text{i}, L_\text{BR}, L_\text{ripple}) \ll \max(\Gamma, \mu)$:

$$\Gamma_\text{s} = \Gamma_\text{s,i} + \Gamma_\text{s,BR} + \Gamma_\text{s,ripple}. \qquad (3)$$

The contributions from the intrinsic ($\Gamma_\text{s,i}$), BR ($\Gamma_\text{s,BR}$), and ripple ($\Gamma_\text{s,ripple}$) relaxation rates are obtained using the Mori-Kawasaki formula similar to that used in ref. [24] considering the conical band structure and the K, K' degeneracy:

$$\Gamma_\text{s,i} = \delta_{\nu,\parallel}\frac{L_\text{i}^2 \arctan(\mu/\Gamma)}{2\pi\mu \cdot \widetilde{\mu}(\mu,\Gamma)}\Gamma, \qquad (4)$$

$$\Gamma_\text{s,BR} = \frac{(2\delta_{\nu,\perp} + \delta_{\nu,\parallel})\,L_\text{BR}^2}{16\pi\widetilde{\mu}(\mu,\Gamma)}\left[1 + \left(\frac{\mu}{\Gamma} + \frac{\Gamma}{\mu}\right)\arctan\left(\frac{\mu}{\Gamma}\right)\right], \qquad (5)$$

$$\Gamma_\text{s,ripple} = \frac{(2\delta_{\nu,\perp} + \delta_{\nu,\parallel})\,\pi}{32}L_\text{ripple}^2\rho(\mu,\Gamma), \qquad (6)$$

$\nu = \parallel$, or $\perp$ is the spin polarization direction with respect to the graphene plane; *e.g.* $\nu = \parallel$ in the spin transport experiments [6]. Here, μ is the chemical potential and $\widetilde{\mu}(\mu,\Gamma) = -\frac{\Gamma}{\pi}\ln(\frac{\mu^2+\Gamma^2}{D^2}) + |\mu|(1 - \frac{2}{\pi}\arctan(\frac{\Gamma}{|\mu|}))$ is the pseudo chemical potential ($D \approx 3\,\text{eV}$ is the cutoff in the continuum theory) which appears in the expression of the density of states (DOS), $\rho(\mu,\Gamma)$, with finite μ and Γ:

$$\rho(\mu,\Gamma) = \frac{2A_\text{c}\widetilde{\mu}(\mu,\Gamma)}{\pi\hbar^2 v_\text{F}^2} \qquad (7)$$

with $A_\text{c} = 5.24\,\text{Å}^2/(2\,\text{atoms})$ being the elementary cell and $\rho(\mu,\Gamma)$ is measured in units of states/eV · atom.

The intrinsic contribution disappears when spins are polarized perpendicular to the plane and the BR and ripple terms have a 2:1 anisotropy for the $\perp$:$\parallel$ directions. For the intrinsic part, $\Gamma_\text{s,i} \approx \frac{L_\text{i}^2}{(2\mu)^2}\Gamma$ when $\mu \gg \Gamma$, which is an Elliott-Yafet–like result with $\alpha_\text{i} = 1$ since the band-band separation, $\Delta = 2\mu$. In the vicinity of the Dirac point, DP, (*i.e.* $\mu \approx 0$ and Γ finite) it returns a Dyakonov-Perel–like result of $\Gamma_\text{s,i} = \frac{L_\text{i}^2}{4\ln(D/\Gamma)}\frac{1}{\Gamma}$. This is in agreement with the generalized Elliott-Yafet theory which predicts a similar crossover when the momentum scattering rate overcomes other energy scales [13]. Interestingly, the intrinsic contribution can be well fitted with a Lorentzian: $\Gamma_\text{s,i} \approx \alpha'\frac{L_\text{i}^2\Gamma'}{\mu^2+\Gamma'^2}$, where $\alpha' \approx 0.2, \ldots, 0.4$ and $\Gamma'/\Gamma \approx 1, \ldots, 2$ for typical values of μ and Γ.

The BR term is only present if a perpendicular electric field, E, is applied, which induces a BR SOC of $L_\text{BR} = \kappa E$ with κ values between 10 [15] and $36\,\mu\text{eV}/(\text{V/nm})$ [14]. The electric field changes μ through: $\mu = \sqrt{n\pi\hbar^2 v_\text{F}^2}$, where $n = \beta E$ is the carrier density and $\beta = 0.22\,(\text{V} \cdot \text{nm})^{-1}$ for SiO_2 gate insulator [25]. This yields the BR SOC as a function of μ: $L_\text{BR}(\mu) \approx \kappa\mu^2 \cdot 3.4\frac{\text{V}}{\text{eV}^2\text{nm}}$.

The ripple relaxation contribution depends on Γ only if $\mu \ll \Gamma$, where it resembles an EY relaxation: $\Gamma_\text{s,ripple} \propto L_\text{ripple}^2\Gamma\ln(D/\Gamma)$. We note however, that the calculation does not include the change of the local graphene coordinates due to the ripples. The deformation of graphene intermixes the z and x, y coordinates which can lead to a significant modification of the anisotropy such as observed experimentally [7].

Analysis of the spin transport data. – In the following, we analyze the available spin transport data [6,7,19] in the framework of the above calculation. Values of $\tau_s = 60, \ldots, 125\,\text{ps}$ were found around the charge neutrality point (depending on the sample), with a typical $\Gamma \approx 75\,\text{meV}$ [19]. Figure 1 shows the measured and calculated spin relaxation rate data for $\nu = \parallel$. $\Gamma = 75\,\text{meV}$, that is independent of μ, was used for the calculated curves. First-principles calculations of the intrinsic SOC scatter more than two orders of magnitude with values of $0.9\,\mu\text{eV}$ [14,26,27]), $24\,\mu\text{eV}$ [15], and $200\,\mu\text{eV}$ [16].
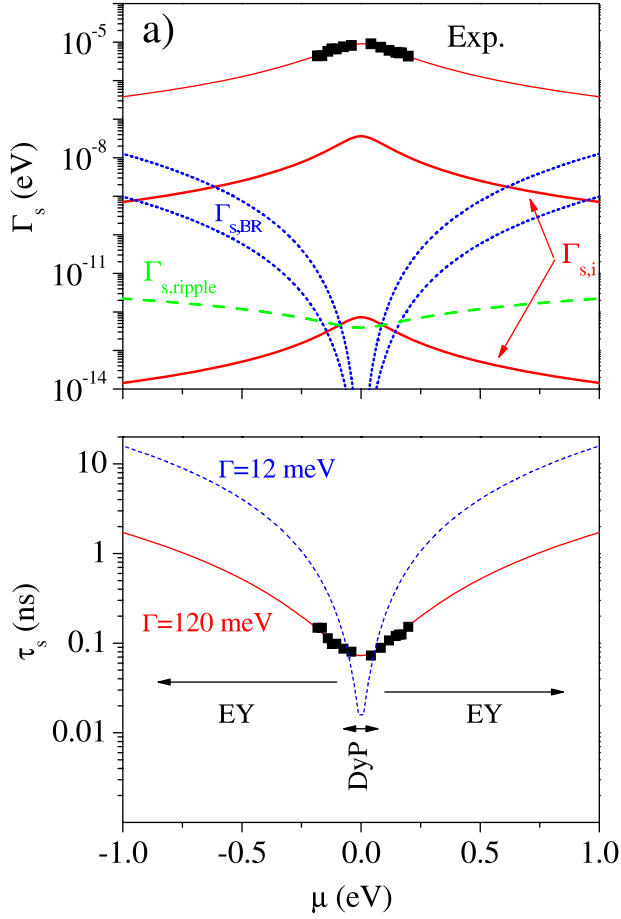
Fig. 1: (Color online) a) Experimental (symbols, from ref. [19]) and calculated spin-lattice relaxation rates, Γ_s, as a function of μ in graphene for in-plane spin polarization. Upper (lower) solid and dotted curves are the maximal (minimal) estimates for the intrinsic and BR contributions with SOC values from refs. [14–16], respectively. The dashed curve is the ripple contribution with L_{ripple} from ref. [14]. The upmost thin solid line is a fit to the data as explained in the text. b) The same experimental data shown as τ_s along with the fit (solid curve). For comparison, τ_s calculated with $\Gamma = 12\,\text{meV}$ (dashed curve) is shown. Arrows depict the crossover of the DyP and EY mechanisms as a function of μ.

Values for the BR SOC, $L_{BR} = \kappa E$, vary between $\kappa = 10, \ldots, 36\,\mu\text{eV}/(\text{V/nm})$. This gives rise to the minimal and maximal estimates for both types of the contributions as shown in fig. 1. The ripple SOC was estimated to be $17\,\mu\text{eV}$ in ref. [14].

Clearly, the first-principles–based relaxation rates fall short of explaining the experimental observation. Of the three contributions, only the intrinsic one has a μ-dependence that mimics the experiment, whereas the other two shows the opposite. It may appear that a fit to the data is ill defined, given the relatively large number of free parameters (Γ and $3\,L$'s). However to our surprise, the fit consistently yields the same, *robust* set of parameters, irrespective of starting values or the method used (least-squares fitting or combined with a simulated

annealing), which are: $L_i = 3.7(1)\,\text{meV}$, $L_{BR} = L_{ripple} = 0$, $\Gamma = 120(5)\,\text{meV}$. This robustness originates from the qualitative difference between the μ-dependence of the different contributions. The obtained values satisfy the criterion for the perturbative approach and the value of Γ determined herein is in agreement with that obtained in ref. [19].

The intrinsic SOC opens a bandgap of L_i in the excitation spectrum [15,16] therefore it is natural to ask: why is not this gap observed experimentally? Two interrelated answers are in order: first, best-quality samples to date are ballistic only on the (sub)micron scale, giving a momentum scattering rate of the order of meV's (or bigger), which can mask the gap [28]. Second, charge inhomogeneities (the so-called puddles) prevent us from reaching the Dirac point, the average minimal charge density is estimated [29] as $10^9\,\text{cm}^{-2}$, which gives an average $\mu \sim 4\,\text{meV}$, capable of overwhelming the obtained gap.

The present analysis allows for the design of graphene-based spintronic devices. For spins polarized perpendicular to the graphene plane, the intrinsic contribution vanishes thus resulting in a substantially longer spin relaxation time. For spins polarized in the graphene plane, fig. 1. shows that around the Dirac point purer samples (*i.e.* smaller Γ) decreases τ_s rather than increasing it, thus deteriorating performance. This, somewhat counterintuitive phenomenon, is the consequence of the Dyakonov-Perel–like behavior of the intrinsic contribution around the DP.

The large value obtained for the intrinsic SOC is surprising as it is an order of magnitude larger than the largest theoretical estimate [16] and up to 3 orders of magnitude larger than other results [14,26,27]). However, given that the experimental μ-dependence of Γ_s dictates the dominant role of the intrinsic coupling, L_i yields necessarily a large value. In the following, we consider two similar systems, MgB_2 and Li-doped graphite and show that therein similar values of the intrinsic coupling are obtained.

In MgB_2, the boron atoms form a honeycomb lattice with four p-shell electrons, such as in graphene, which highlights the similarity of the two materials. Therein, an intrinsic SOC of $L_i(MgB_2) = 2.8\,\text{meV}$ of the π-orbitals was found [24]. It was shown by Grüneis and coworkers [30] and confirmed [31] that alkali-atom–intercalated graphite is an excellent model system of biased graphene as the two-dimensional electron dispersion is retained due to the weak interlayer coupling. The Li-intercalated stage-I graphite compound LiC_6 [23] is particularly suitable to determine the intrinsic SOC as Li is the lightest alkali metal and its contribution to the spin relaxation is undetectable [4].

In fig. 2, we show the temperature-dependent ESR linewidth, ΔB, for an HOPG LiC_6 along with previous data on a powder LiC_6 sample [32] and schematics of the band structure. A linear fit to the data yields $\Delta B = 0.205\,(\text{mT}) + T \times 6 \cdot 10^{-5}\,(\text{mT/K})$. Of these terms, the temperature-dependent one is associated with the homogeneous broadening, ΔB_{hom}, due to SOC, which
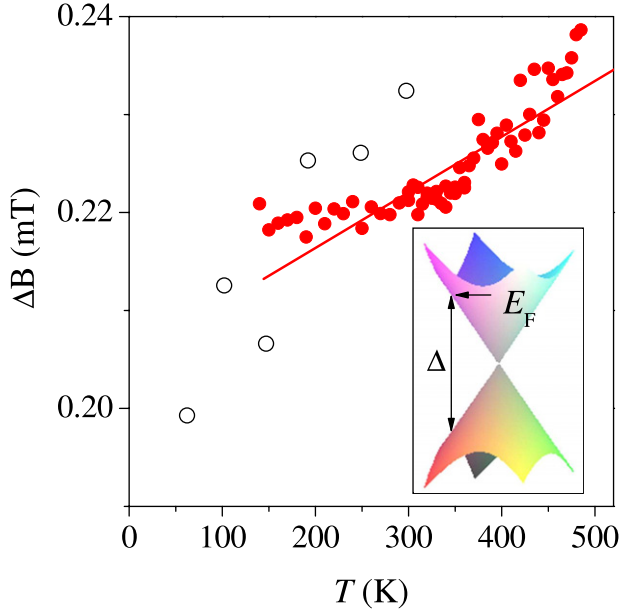
Fig. 2: (Color online) High-temperature ESR linewidth in HOPG LiC_6 (full symbols) and linear fit to the data (solid line). We show similar data from ref. [32] (open symbols) on a LiC_6 powder sample. The inset shows the schematics of the LiC_6 band structure according to the PES measurements [30,31] and the $\Delta = 1.65\,\text{eV}$ parameter.
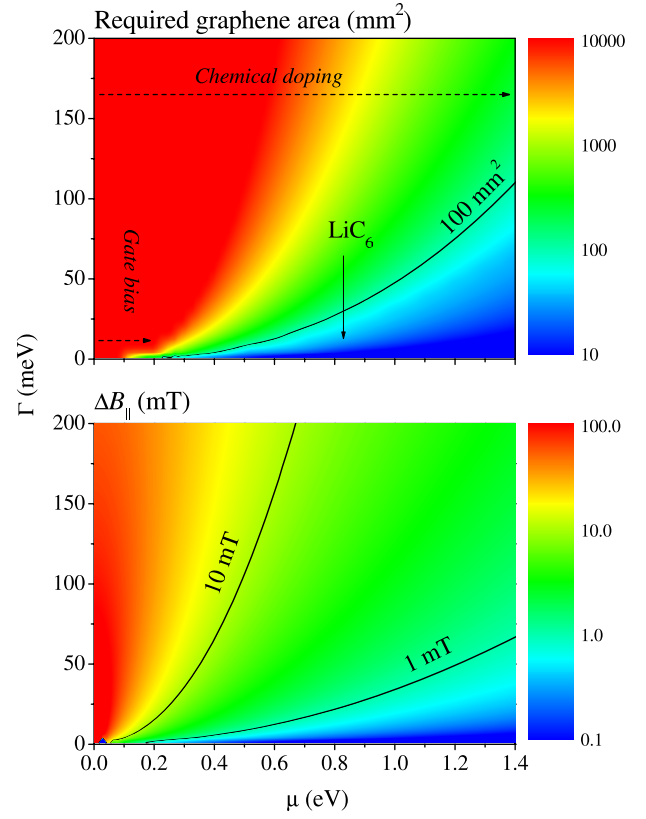

Fig. 3: (Color online) Limit of ESR detection for graphene as a function of μ and Γ in units of the graphene area (upper panel) for an in-plane magnetic field. The arrows show the maximum chemical potential by gate bias and by chemical doping and the solid curve indicates the $100\,\text{mm}^2$ area border. Expected ESR linewidth, $\Delta B_\parallel$ (lower panel), solid lines show two selected linewidths, 1 and $10\,\text{mT}$.

gives $\Gamma_s = g\mu_B \Delta B_{\text{hom}}$ ($g \approx 2$ is the g-factor, μ_B is the Bohr magneton) and is $\Gamma_s = 2.1 \cdot 10^{-9}\,\text{eV}$ at $300\,\text{K}$. Since Li-doped graphite resembles biased graphene [30,31], the above theory of the intrinsic SOC applies, *i.e.* $\Gamma_s = \frac{L_i^2}{\Delta^2}\Gamma$. With the values of $\Delta = 1.65\,\text{eV}$ [31] and a typical $\Gamma(300\,\text{K}) = 4.4\,\text{meV}$ [23], we obtain $L_i(LiC_6) = 1.1\,\text{meV}$. Although it is debated whether SOC in graphite is applicable for graphene [14], the similar result for these three systems leads us to conclude that the intrinsic SOC is properly determined in graphene.

Detectability of ESR on graphene. – With the SOC parameters and the theory of spin relaxation at hand, we assess the feasibility of ESR spectroscopy on graphene. It is determined by the sample amount, the magnitude of the spin-susceptibility, and the ESR linewidth. The ESR signal is proportional to the amount of magnetic moments: $\chi_0 V B/\mu_0$, where B is the magnetic field, χ_0 is the volume spin-susceptibility (dimensionless in SI units), V is the sample volume, and μ_0 is the permeability of vacuum. For graphene with area A, the amount of magnetic moments is $\chi_{0,\text{gr}} A B/\mu_0$ with $\chi_{0,\text{gr}}$ having a unit of meters. The Pauli spin-susceptibility of graphene is $\chi_{0,\text{gr}} = \mu_0\mu_B^2\rho(\mu,\Gamma)\frac{N}{A}$, N is the number of carbons and the DOS, $\rho(\mu,\Gamma)$, is given above.

ESR spectrometer performance is given by the limit-of-detection (LOD_0) *i.e.* the number of $S = 1/2$ non-interacting spins at $300\,\text{K}$ which give a signal-to-noise of $S/N = 10$ ratio for $\Delta B = 0.1\,\text{mT}$ linewidth, and $1\,\text{s/spectrum-point}$ time constant. For state-of-the-art

spectrometers $\text{LOD}_0 = 10^{10}$ spins/$0.1\,\text{mT}$. The spin-susceptibility of such spins is $\chi_{\text{Curie}} = \mu_0\mu_B^2\frac{N_s}{V}/(k_B T)$, where N_s spins occupy a volume of V, which gives an LOD for graphene:

$$\text{LOD}_{\text{gr}} = \text{LOD}_0 \cdot \frac{f(\Delta B)}{26\,\text{meV} \times \rho(\mu,\Gamma)} \qquad (8)$$

in units of number of carbons. Here, $26\,\text{meV}$ is the thermal energy at $300\,\text{K}$ and the $f(\Delta B = 0.1\,\text{mT}) = 1$ function describes that the ESR S/N decreases as $1/\Delta B$ if $\Delta B < 1\,\text{mT}$ (the typical magnetic-field modulation limit) and as $1/(\Delta B)^2$ if $\Delta B \geqslant 1\,\text{mT}$. For $\mu > \Gamma$, the DOS is well approximated by $\rho(\mu) = 0.0385\mu \cdot (\text{states/eV}^2\,\text{atom})$ which yields a compact result: $\text{LOD}_{\text{gr}} \approx 1000\,\text{LOD}_0 \cdot f(\Delta B)/\mu$ with μ in eV units.

Clearly, a sizeable DOS and narrow linewidth are prerequisites to observe ESR on graphene. Large DOS can be achieved by moving μ away from the DP or by inducing defects. The latter yields, however, increased scattering thus larger linewidth. Shifting μ by a gate bias is limited to $\sim 0.2\,\text{eV}$ due to breakdown in the most common SiO_2 insulator around $E \approx 0.1\,\text{V/nm}$. With chemical doping using K, up to $\mu \sim 1.35\,\text{eV}$ can be achieved [30]. The ESR

linewidth is expected to be strongly anisotropic with a minimum, $\Delta B_\perp$, for a perpendicular magnetic field, its magnitude however remains unknown. In fig. 3, we show the calculated LOD for graphene as a function of μ and Γ in units of the graphene area along with the calculated linewidth for an in-plane magnetic field. The LOD can be two orders of magnitude smaller for a perpendicular magnetic field if the corresponding ESR linewidth is an order of magnitude smaller. Therefore ESR experiments should be attempted with the perpendicular orientation first. This experiment would yield directly the magnitude of the BR and ripple relaxation contributions from $\Delta B_\perp$.

An important benchmark, that indeed the intrinsic ESR signal of graphene is observed, is the angular dependence of the ESR linewidth: $\Delta B(\theta) = \sin^2(\theta)\Delta B_\parallel + \cos^2(\theta)\Delta B_\perp$ as a function of the asimuth angle, θ. Finally, we note that the anisotropy could reconcile the narrow ESR linewidth in the perpendicular geometry [21] with the short τ_s in the spin transport experiment [6].

In conclusion, we presented a theory of spin relaxation in graphene which takes into account intrinsic, Bychkov-Rashba, and ripple spin-orbit coupling-induced spin relaxation. The analysis of spin relaxation data shows that the intrinsic contribution dominates the relaxation with a coupling constant that is orders of magnitude larger than theoretical estimates but it is not unusually large compared to other honeycomb systems. The result predicts a large anisotropy of the spin relaxation. We presented under what circumstances bulk ESR spectroscopy can be observed in graphene.

$$* * *$$

REFERENCES

[1] NOVOSELOV K. S., GEIM A. K., MOROZOV S. V., JIANG D., ZHANG Y., DUBONOS S. V., GRIGORIEVA I. V. and FIRSOV A. A., *Science*, **306** (2004) 666.

[2] ŽUTIĆ I., FABIAN J. and SARMA S. D., *Rev. Mod. Phys.*, **76** (2004) 323.

[3] BOLOTIN K. I., SIKES K. J., JIANG Z., KLIMA M., FUDENBERG G., HONE J., KIM P. and STORMER H. L., *Solid State Commun.*, **146** (2008) 351.

[4] BEUNEU F. and MONOD P., *Phys. Rev. B*, **18** (1978) 2422.

[5] FORRÓ L., SEKRETARCZYK G., KRUPSKI M., SCHWEITZER D. and KELLER H., *Phys. Rev. B*, **35** (1987) 2501.

[6] TOMBROS N., JÓZSA C., POPINCIUC M., JONKMAN H. T. and VAN WEES B. J., *Nature*, **448** (2007) 571.

[7] TOMBROS N., TANABE S., VELIGURA A., JÓZSA C., POPINCIUC M., JONKMAN H. T. and VAN WEES B. J., *Phys. Rev. Lett.*, **101** (2008) 046601.

[8] ELLIOTT R. J., *Phys. Rev.*, **96** (1954) 266.

[9] YAFET Y., *Solid State Phys.*, **14** (1963) 1.

[10] DRESSELHAUS G., *Phys. Rev.*, **100** (1955) 580.

[11] BYCHKOV Y. A. and RASHBA E. I., *J. Phys. C*, **17** (1984) 6039.

[12] BYCHKOV Y. A. and RASHBA E. I., *JETP Lett.*, **39** (1984) 78.

[13] DÓRA B. and SIMON F., *Phys. Rev. Lett.*, **102** (2009) 137001.

[14] HUERTAS-HERNANDO D., GUINEA F. and BRATAAS A., *Phys. Rev. B*, **74** (2006) 155426.

[15] GMITRA M., KONSCHUH S., ERTLER C., AMBROSCH-DRAXL C. and FABIAN J., *Phys. Rev. B*, **80** (2009) 235431.

[16] KANE C. L. and MELE E. J., *Phys. Rev. Lett.*, **95** (2005) 226801.

[17] ERTLER C., KONSCHUH S., GMITRA M. and FABIAN J., *Phys. Rev. B*, **80** (2009) 041405.

[18] CASTRO NETO A. H. and GUINEA F., *Phys. Rev. Lett.*, **103** (2009) 026804.

[19] JÓZSA, MAASSEN T., POPINCIUC M., ZOMER P. J., VELIGURA A., JONKMAN H. T. and VAN WEES B. J., *Phys. Rev. B*, **80** (2009) 241403(R).

[20] GRISWOLD T. W., KIP A. F. and KITTEL C., *Phys. Rev.*, **88** (1952) 951.

[21] CIRIC L., SIENKIEWICZ A., NÁFRÁDI B., MIONIC M., MAGREZ A. and FORRÓ L., *Phys. Status Solidi B*, **246** (2009) 2558.

[22] ZANINI M., BASU S. and FISCHER J. E., *Carbon*, **16** (1978) 211.

[23] DRESSELHAUS M. S. and DRESSELHAUS G., *Adv. Phys.*, **51** (2002) 1.

[24] SIMON F., DÓRA B., MURÁNYI F., JÁNOSSY A., GARAJ S., FORRÓ L., BUD'KO S., PETROVIC C. and CANFIELD P. C., *Phys. Rev. Lett.*, **101** (2008) 177003.

[25] FERNÁNDEZ-ROSSIER J., PALACIOS J. J. and BREY L., *Phys. Rev. B*, **75** (2007) 205441.

[26] MIN H., HILL J. E., SINITSYN N. A., SAHU B. R., KLEINMAN L. and MACDONALD A. H., *Phys. Rev. B*, **77** (2006) 165310.

[27] YAO Y., YE F., QI X.-L., ZHANG S.-C. and FANG Z., *Phys. Rev. B*, **75** (2007) 041401.

[28] CASTRO NETO A. H., GUINEA F., PERES N. M., NOVOSELOV K. S. and GEIM A. K., *Rev. Mod. Phys.*, **81** (2009) 109.

[29] FELDMAN B. E., MARTIN J. and YACOBY A., *Nat. Phys.*, **5** (2009) 889.

[30] GRÜNEIS A., ATTACCALITE C., RUBIO A., VYALIKH D. V., MOLODTSOV S. L., FINK J., FOLLATH R., EBERHARDT W., BÜCHNER B. and PICHLER T., *Phys. Rev. B*, **80** (2009) 075431.

[31] PAN Z.-H., CAMACHO J., UPTON M., FEDOROV A., WALTERS A., HOWARD C., ELLERBY M. and VALLA T., *Why is KC_8 a superconductor and LiC_6 is not?* arXiv:1003.3903.

[32] LAUGINIE P., ESTRADE H., CONARD J., GUÉRARD D., LAGRANGE P. and EL MAKRINI M., *Physica B*, **99** (1980) 514.